Hydrothermal mounds and young ocean crust of the Galapagos: Preliminary Deep Sea Drilling results, Leg 70

JOSE HONNOREZ *School of Marine and Atmospheric Sciences, University of Miami, 4600 Rickenbacker Causeway, Miami, Florida 33149*
RICHARD P. VON HERZEN *Department of Geology and Geophysics, Woods Hole Oceanographic Institution, Woods Hole, Massachusetts 02543*

TIMOTHY J. BARRETT *Institut und Museum fur Geologie und Palaontologie, Universitat Tubingen, 7400 Tubingen 1, Sigwartstrasse 10, Federal Republic of Germany*
KEIR BECKER *Marine Physical Laboratory A-005, Scripps Institution of Oceanography, La Jolla, California 92093*
MICHAEL L. BENDER *Graduate School of Oceanography, University of Rhode Island, Kingston, Rhode Island 02881*
PETER E. BORELLA *Deep Sea Drilling Project A-031, Scripps Institution of Oceanography, La Jolla, California 92093*
HANS-WOLFGANG HUBBERTEN *Institut fur Petrographie u. Geochemie der Universitat, 75 Karlsruhe 1, Kaiserstr. 12, Federal Republic of Germany*
STEVEN C. JONES *Department of Geology, Florida State University, Tallahassee, Florida 32306*
SHUN'ICHIRO KARATO *Ocean Research Institute, University of Tokyo, Nakano, Tokyo 164, Japan*
CHRISTINE LAVERNE *Laboratoire de Geologie, Faculte des Sciences et Techniques, BP W SFAX Tunisie, France*
SHAUL LEVI *School of Oceanography, Oregon State University, Corvallis, Oregon 97331*
AREG A. MIGDISOV *Vernadsky Institute of Geochemistry and Analytical Chemistry, U.S.S.R. Academy of Sciences, Moscow, U.S.S.R.*
S. ANTHONY MOORBY *Department of Geology, Imperial College, London SW7 2BP, United Kingdom*
ED L. SCHRADER *Department of Geology and Geography, University of Alabama, P.O. Box 1945, University, Alabama 35486*

ABSTRACT

A total of 32 holes at 5 sites near 1°N, 86°W drilled on Deep Sea Drilling Project (DSDP) Leg 70 (November–December 1979) provide unique data on the origin of the hydrothermal mounds on the south flank of the Galapagos spreading center. Hydrothermal sediments, primarily Mn-oxide and nontronite, are restricted to the immediate vicinity of the mounds (≤100 m) and are probably formed by the interaction of upward-percolating hydrothermal solutions with sea water and pelagic sediments above locally permeable zones of ocean crust. Mounds as much as 25 m in height form in less than a few x 10^5 yrs, and geothermal and geochemical gradients indicate that they are actively forming today. The lack of alteration of upper basement rocks directly below the mounds and throughout the Galapagos region indicates that the source of the hydrothermal solutions is deeper in the crust.

INTRODUCTION AND BACKGROUND

Interaction between the oceanic crust and sea water at or near active spreading centers is one of the most influential post-eruptive processes controlling the evolution of the oceanic lithosphere. Circulation of sea water through the oceanic crust is thought to effectively cool young crustal material. During sea-water–basalt interaction at above-ambient temperatures, intense but probably localized chemical reactions and mineralogical changes occur which alter the composition of the crust, the overlying sediments, and the sea water itself (Edmond and others, 1979a, 1979b and ref. therein). Hydrothermal reactions are believed to significantly change the chemical and physical properties of seismic Layer 2 (Houtz and Ewing, 1976; Ewing and Houtz, 1979 and ref. therein). Finally, metallogenetic processes are closely related to this interaction and they are thought to be similar to those which generate many base metal ore deposits.

Leg 70 of the Deep Sea Drilling Project was dedicated to the over-all study of the hydrothermal interaction between oceanic crust, sea water, and overlying sediments from the geophysical, geochemical, and petrological points of view. Particularly emphasized on Leg 70 was the study of a very young, "open," hydrothermal system close to the actively spreading Galapagos ridge, in contrast to a somewhat older, partly "closed" system on a segment of the Costa Rica rift investigated on Legs 68, 69, and 70 (CRRUST, 1981).

The Galapagos spreading center is one of the best-surveyed regions of the deep-sea floor. Heat-flow measurements (Sclater and Klitgord, 1973; Sclater and others, 1974; Williams and others, 1974; Green and others, 1981), bathymetric surveys (Hey and others, 1977; Lonsdale, 1977; Allmendinger and Riis, 1979), magnetic profiles (Sclater and Klitgord, 1973; Klitgord and Mudie, 1974), and samples from the hydrothermal vents (Corliss and others, 1979a, 1979b; Edmond and others, 1979a, b) show that the Galapagos spreading center has been active and is a site of intense hydrothermal activity. The half spreading rate, calculated from the magnetic anomalies, has been about 3.5 cm/10^3 yr for the past 2.0 m.y. Although we lacked detailed seismic data on the thickness of the sediment cover in the region south of the Galapagos spreading center, profiles show that the sediment cover increases rapidly and regularly away from the spreading axis. The region south of the Galapagos spreading center is characterized by a regularly varying heat-flow pattern, strongly lineated subparallel to the spreading axis.

A subtle and thus far unique feature discovered during surveys with deep-towed

Geological Society of America Bulletin, Part I, v. 92, p. 457–472, 8 figs., 4 tables, July 1981.

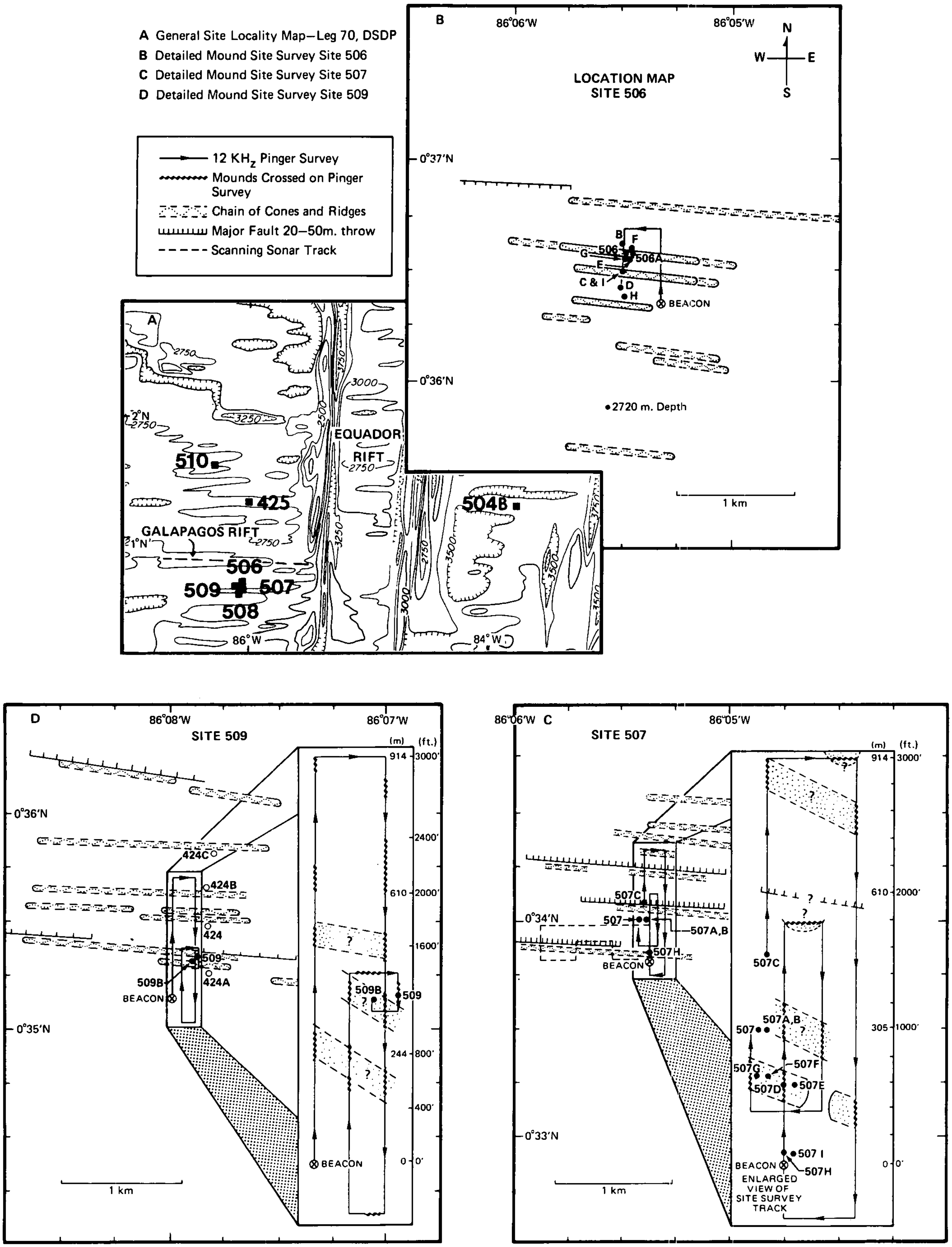

Figure 1. Index map and detailed mounds surveys of Sites 506, 507, and 509.

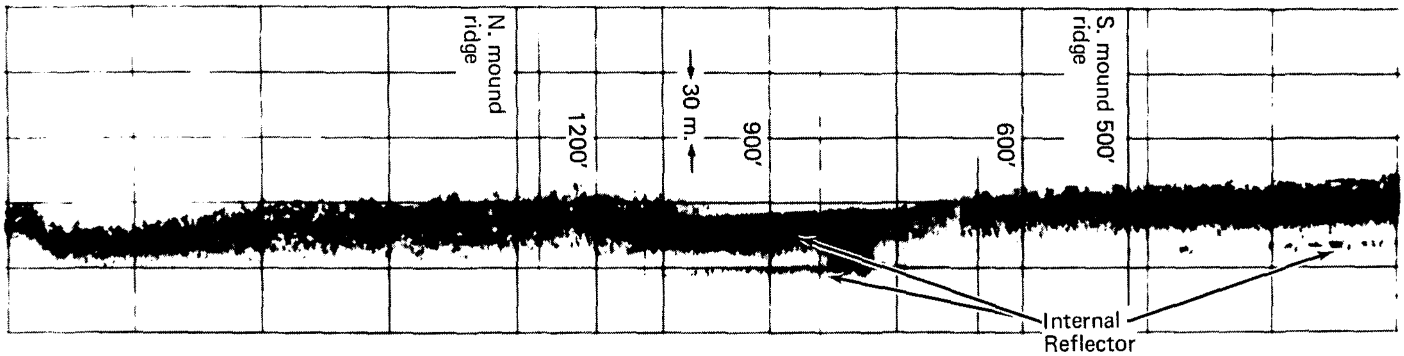

Figure 2. Record of portion of 12-kHz pinger survey, Site 506. Note lack of internal reflectors beneath the mound ridges.

geophysical equipment, and later sampled by the submersible *Alvin,* is the presence of hydrothermal mounds south of the spreading axis (Klitgord and Mudie, 1974; Lonsdale, 1977; Corliss and others, 1979a; Williams and others, 1979). The mounds often occur as more or less continuous chains, oriented sub-parallel to the spreading axis. They sometimes appear to be located above small vertical displacements in basement rock, presumably fracture controlled, also oriented subparallel to the axis. The mounds are from 5 to 20 m higher than the general level of the adjacent sea floor and are often surrounded by a shallow moat less than 5 m deep. They are 25 to 100 m across at their bases, and their slopes are generally steep, as much as 45°. The mound surfaces are generally dark colored with local bright yellow spots and bands in comparison with the surrounding light tan or gray pelagic oozes (Williams and others, 1979).

The seismic reflectors found at subbottom depths of about 7 and 15 m over much of the region south of the Galapagos spreading center were tentatively ascribed by Lonsdale (1977) to the presence of ash layers, deposited about 140,000 and 300,000 yr ago, respectively. One objective of drilling was to determine the nature of these reflectors and to establish the validity of the Leg 54 scientific party suggestion that these reflectors are to be ascribed to the regional extension of hydrothermal sediments centered at the mounds (Natland and others, 1979). *In situ* measurements and drill samplings were carried out in a series of environments characterized by high conductive heat flow, with and without hydrothermal "mounds," and in relatively low heat-flow areas nearby. Another objective was the recovery of basement rocks from beneath the mounds and their environs to determine the nature and extent of rock alteration. Drilling of basement rocks proved difficult on Leg 54 (Natland and others, 1979), and such was the case also on Leg 70, with a maximum penetration of 19 and 7.2 m of basalt recovered at Site 510 (Fig. 1).

In preparation for drilling the mounds, detailed site surveys were made in the mounds fields (Fig. 1). Using a 12-kHz pinger attached to the drill string ~ 100 m above the drill bit, the mounds frequently appeared as diffuse echoes elevated 5 to 10 m above the sea floor, as much as 100 m wide. Their seismic profile is characterized by a disappearance of internal reflectors beneath them (Fig. 2). A sonar scanning tool developed for hole re-entry was also used to help locate the mounds. It gave a broader view of the mounds ridges than the 12-kHz drill string pinger, confirming the lineations of the mound ridges and showing individual mounds peaks comprising the ridges. After mapping of the mound ridges with ship navigation controlled by a bottom-mounted beacon, the drill pipe was successfully positioned over desired sites with a lateral precision estimated at about 20 m. Such precision allowed drilling of mounds with widths of 50 to 100 m, although an uncertainty of the order of 20 m with respect to the mound axes must exist.

A newly developed hydraulic piston corer (HPC) was used quite successfully at all sites. Recovery was high, averaging 93% of the cored section, with most of the cores showing detailed and undisturbed stratigraphy. A useful by-product of the deployment of the 12-kHz drill string pinger is the ability to place the drill bit within 1 to 2 m of the sea floor, thereby ensuring recovery of "mud line" sediments on the first coring attempt.

SEDIMENTS

Sedimentology

The sediments recovered on Leg 70 can be divided into two major classes: *Hydrothermal sediments* are found only in the holes drilled on, or in the close vicinity of, mounds (506, 506C, 506D, 507D, 507F, 509B; see Fig. 1). These sediments are subdivided into manganese oxide crust fragments and green nontronitic clays. *Pelagic sediments,* basically nannofossil oozes, are found in all the holes cored. They are further subdivided on the basis of the amount of calcareous and siliceous microfossils present.

Hydrothermal Sediments. *Manganese Oxide Crusts.* Such crusts were not recovered from every site in the vicinity of mounds. Where they occur, they are the uppermost hydrothermal sediment and are overlain by 7 cm to 1.4 m of pelagic sediment. The greatest thickness of manganese crust fragments (1.4 m) was recovered from Hole 509B; at the other holes, the thickness is apparently only from a few centimetres to tens of centimetres.

The managanese-oxide crusts consist of brownish-black, pebble- to granule-sized, flat, angular, and occasionally saucer-shaped fragments. Their surface texture varies from smooth to botryoidal and granular. X-ray diffraction analysis showed that the major mineral present is todorokite. In one thin section of porous Mn crust, limonite occurs in irregularly bounded zones or rings which are surrounded by todorokite (Fig. 3A).

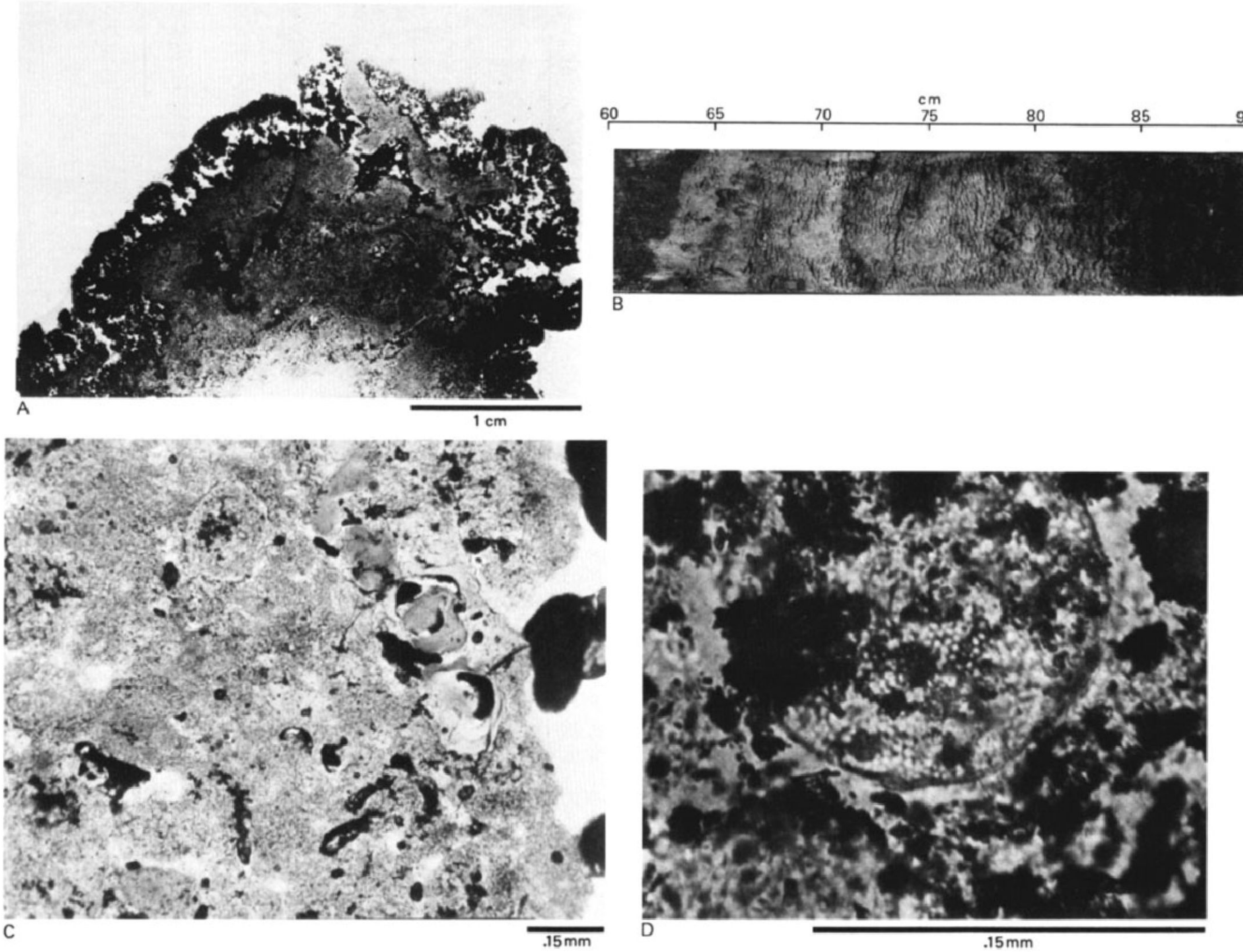

Figure 3. Photographs of sediments of the Galapagos hydrothermal mounds. See text for identification.

Green Nontronitic Clay. The overwhelming majority of recovered hydrothermal sediment is essentially composed of nontronite. Megascopically, the nontronite is green to greenish-black and forms semiconsolidated angular aggregates ranging from less than 1 mm to 20 mm in size (Fig. 3B). Although nontronite generally forms such a coarse granular sediment, it occasionally takes on a finer-grained, nongranular, and more compact appearance. The nongranular nontronite sediment is slightly lighter in color, and usually shows a gradational contact with the coarse-granular variety or with pelagic sediments.

Microscopically, the nontronite is green to yellowish-brown or brown in color, fine silt to sand in size, and sub-equant to irregular in shape (Fig. 3C). Impregnated thin sections of the nontronitic clay show occasional examples of calcareous and siliceous microfossils which appear to be wholly or partially replaced by nontronite (Fig. 3D). Calcareous microfossils are rare, with the estimated total carbonate content in the nontronitic layers being less than 2%. Some smear slides of green nontronite show foraminifers which may have been infilled, coated, or possibly replaced by green nontronite.

Pelagic Sediments. The pelagic sediments are primarily composed of calcareous nannofossils, foraminifers, diatoms, radiolaria, and silicoflagellates. Three different types of nannofossil-rich oozes are recognized on the basis of microfossil assemblages. Using the standard DSDP sediment classification (Ross, Neprochnov, and others, 1978), these are: (a) foraminifer nannofossil ooze, (b) siliceous foraminifer nannofossil ooze, and (c) diatom-nannofossil ooze.

The nannofossil oozes are multicolored, with a dominant greenish-gray to light greenish-gray color. For some 20 to 50 cm below the sediment water interface, these oozes are moderate brown in color, probably as a result of disseminated MnO_2 (Lynn and Bonatti, 1965). The greenish-gray oozes are extensively mottled due to burrowing organisms. Excellent examples of *Zoophycus, Planolites* and *Halo burrows*(?) are present. Many intensely mottled sections of both near-mounds and off-mounds cores contain green nontronitic clay. This implies that limited amounts of nontronitic clay may have precipitated in the off-mounds areas or that the mottles may be included fragments of slumped material from nearby mounds. No other direct evidence of slumping was observed.

Preservation of microfossils varies from site to site. The non-mounds sites (508 and 510) show much better preservation of microfossils than do the mounds sites (506, 507, and 509). Calcareous nannofossils

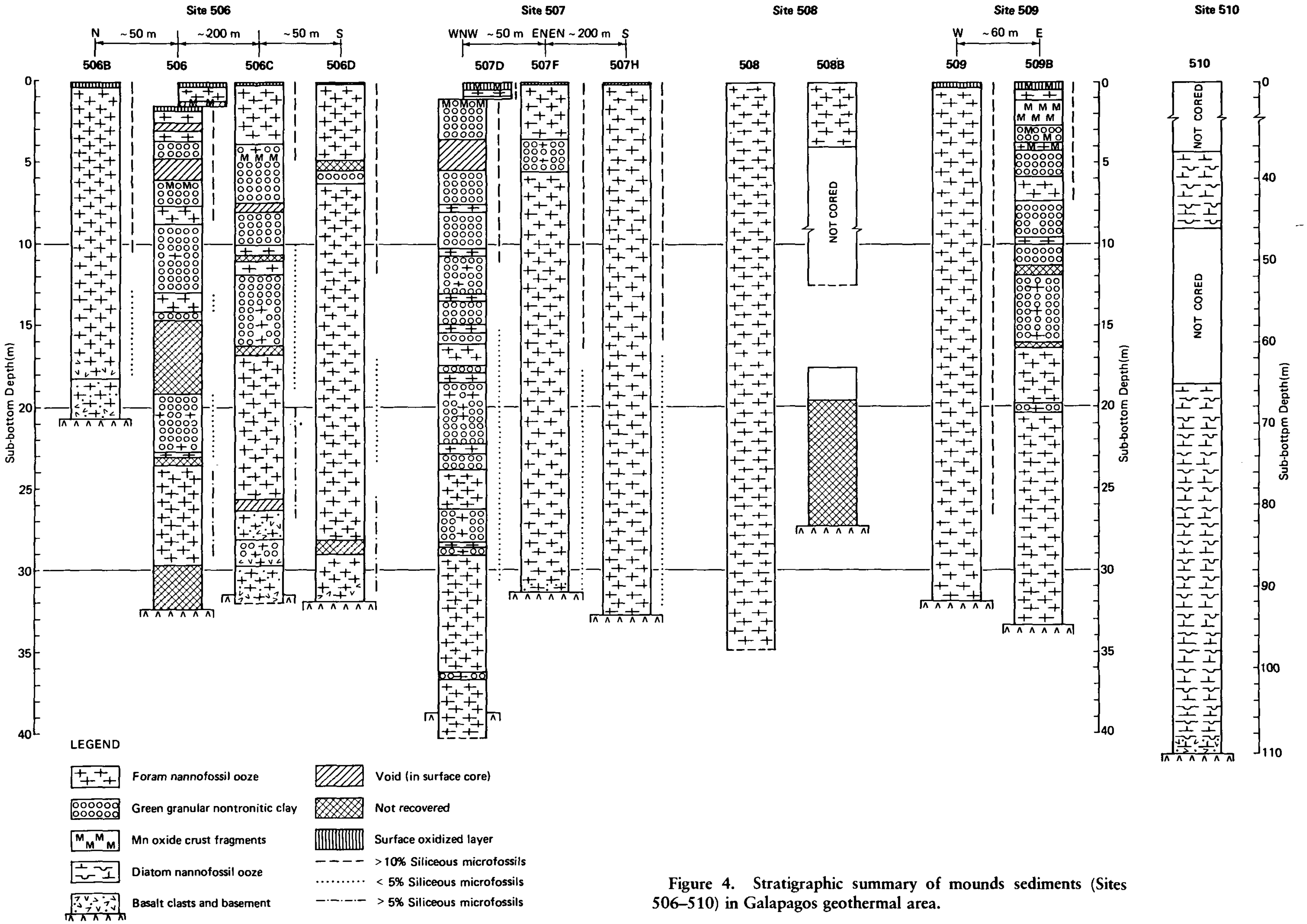

Figure 4. Stratigraphic summary of mounds sediments (Sites 506–510) in Galapagos geothermal area.

identified in the basal sediments at Sites 506, 507, 508, and 509 were late Pleistocene (0.27 to 0.55 m.y. B.P.) in age and were assigned to the *Gephyrocapsa oceanica* Zone (Martini, 1971; Gartner, 1977). Planktonic foraminifers substantiate this age (Kaneps, 1971), but no zonal assigment was possible.

The basal sediments recovered at Site 510 were early Pliocene (2.6 to 3.0 m.y. B.P.) in age. The planktonic foraminifers were assigned to the *Globorotalia limbata* Zone and the calcareous nannofossil to the *Reticulofenestra pseudoumbilica* Zone. This age assignment is in good agreement with the crustal magnetic anomaly age of 2.73 m.y. B.P.

Stratigraphy

The stratigraphic relationships of the sediments cored in the Galapagos area are presented in Figure 4. Each mound sediment column can be subdivided into three stratigraphic units (proceeding from top to bottom): *Unit A:* Upper pelagic oozes, *Unit B:* Interbedded and mixed hydrothermal sediments and pelagic oozes, and *Unit C:* Lower pelagic oozes.

Unit A consists of pelagic oozes with a siliceous component greater than 10%. The upper boundary is defined by the sediment-water interface and the lower boundary by the first occurrence of a hydrothermal sediment layer. The thickness of this unit varies from 0.3 to 3.0 m. Manganese oxide crust fragments are present in several cores within Unit A, but they do not form any definite layer. The lower contact of Unit A with Unit B is sharp in all but one hole.

Unit B, the interbedded and mixed hydrothermal sediment and pelagic ooze interval, ranges in thickness in the near-mound sites from 1 to 28 m. In all but one hole (509B), nontronitic clay comprises the bulk of the uppermost hydrothermal layer. In Hole 509B, a 1.4-m-thick unit of manganese oxide crust fragments forms the uppermost hydrothermal layer. The contacts between interbedded pelagic and hydrothermal sediments within Unit B are gradational, with the more compact green nontronite generally constituting the transitional hydrothermal sediment. Two of the near-mounds holes (506D, 507F) have hydrothermal sediment layers with thicknesses of 1.0 and 2.0 m, respectively; in the others, the range is from 13 to 28 m thick. The hydrothermal sediments which make up the bulk of Unit B are not found farther than about 50 m from the mounds sites.

At the holes with a large thickness (≥13 m) of hydrothermal sediments, the siliceous fossil content in the pelagic component of the sediments always drops below 5% at ~ 8 to 12 m below the sea-water–sediment surface. At holes with minor or no thickness of hydrothermal sediments, this reduction in siliceous fossil content occurs at about 10 m sub-bottom at Site 506, 17 m at Site 507, and 27 m at Hole 509. The reduction is not present in the non-mound Sites 508 and 510 (Fig. 4).

Unit C, the lowermost unit in the mounds area, is composed of foraminifer nannofossil oozes and varies in thickness from 7 to 17 m. The upper contact of this unit with the nontronitic clay is gradational. The lower boundary is the basement-sediment interface. Preservation of burrows is good, with intense mottling occurring immediately beneath the last cohesive layer of nontronite in Unit B and extending downward from 1 to 6 m. These mottles are rich in nontronitic clay. The pelagic sediment immediately overlying the basement is mottle-and nontronite-free.

Pore-Water Chemistry

Our pore-water results reflect the upwelling of hydrothermal solutions throughout the mounds area. Shipboard pore-water sampling on cores was done at *in situ* temperatures, using a Sorvall refrigerated super-speed centrifuge. Comparison with seven *in situ* pore-water samples showed that the Mg and Si concentrations of the centrifuged samples are close to *in situ* values, while Ca concentrations are 0.4 mM less than *in situ* values. The comparison omits two Site 508 *in situ* samples, which are believed to differ in composition from the centrifuged samples as a result of local variability in pore-water chemistry rather than as a sampling artifact. Suboxic squeezing experiments on Leg 70 show that low Si concentrations are not an artifact of Fe^{2+} oxidation during centrifuging (Loder and others, 1978).

Pore-water chemistry is shown in Figure 5 for three contrasting holes: a low heat-flow site (508), a mounds site (509B), and an off-mounds pelagic site (509). Similar results are found at the other holes in this region. The pore-water chemistry reveals the following features:

1. Pore waters at high heat-flow sites (509 and 509B) are enriched in Ca by 0.5 to 2.0 mM and depleted in Mg by 1.5 to 3.0 mM/liter relative to bottom water. At the low heat-flow Site 508, Ca is close to the bottom-water value, and Mg is only slightly depleted (by about 0.6 mM). However, three of the Site 508 samples, including two *in situ* samples taken at 19 and 26 m, show positive Ca and negative Mg anomalies comparable to those at high heat-flow sites. The Ca enrichment and Mg depletion of pore-water samples from high heat-flow sites probably reflect flow through the sediments of sea water which has gained Ca and lost Mg as a result of reaction with basalt. The Ca and Mg concentrations of low heat-flow site samples, being respectively similar to or slightly lower than the values for bottom sea water, are thought to correspond to downward flow of sea water and recharge of the basement aquifer (Williams and others, 1974; Green and others, 1981). The positive Ca and negative Mg anomalies of pore waters at the bottom of low heat-flow Site 508 may reflect diffusive exchange of Ca and Mg out of basalt, superimposed on slow recharge.

2. Si concentrations of pore waters are generally highest in sediments located in low heat-flow regions, reaching 600 μM. These high Si concentrations probably reflect dissolution of biogenic silica near the sediment surface, accompanied by downward advection. The lower Si concentration (between 200 and 400 μM) in high heat-flow regions is probably associated with pore waters which enter the mounds sediments from below and gain biogenic Si as they ascend. This low Si concentration may indicate the presence of Si-depleted formation waters.

3. NH_3 concentrations are highest in pore-water samples from low heat flow sites. These may indicate descent of solutions which pick up NH_3 produced by sulfate reduction near the sediment-water interface and advect it downward. Contrastingly, the pore waters from Hole 509 have gained metabolic ammonia as they rise; the ammonia profile reflects production and downward diffusion against slow upwelling. The low ammonia concentrations in the pore water from Hole 509B reflect rapid convection and perhaps a deficiency of organic matter in the authigenic Mn and Fe compounds and sediments of the mounds.

Physical Properties

Wet bulk density, grain density, porosity, compressional wave velocity, and thermal conductivity of over 200 sediment samples were measured on board D/V *Glomar Challenger.* In Table 1, the means and standard deviations of these measurements are given for the four sediment types recovered. Grain densities and, in general, other physical properties systematically covary among these types in the order in which they are listed; for example, manganese oxides are more dense, have the highest velocities, and

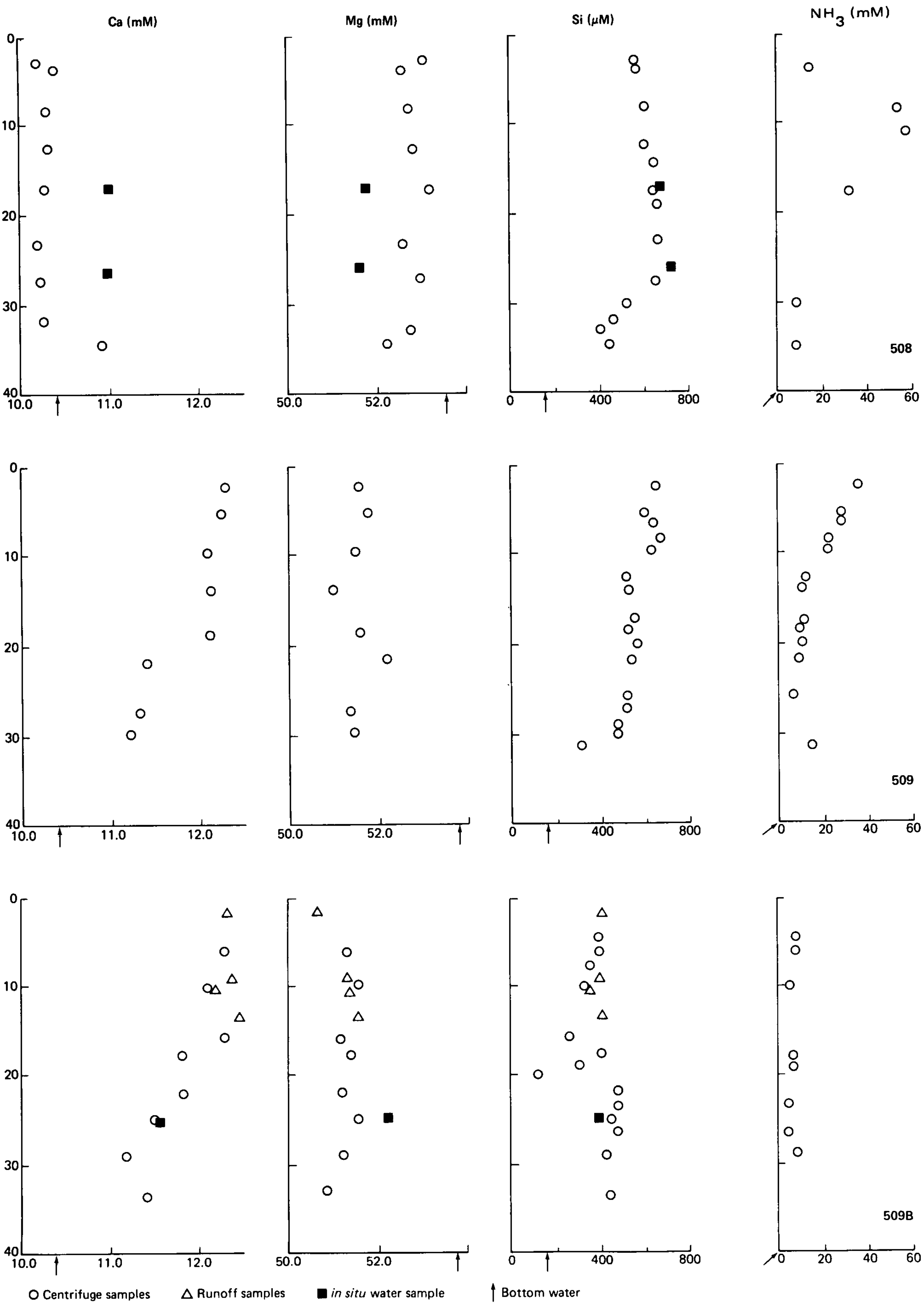

Figure 5. Pore-water chemistry results.

TABLE 1. AVERAGE VALUES OF PHYSICAL PROPERTIES OF SEDIMENTS FROM THE GALAPAGOS AREA, LEG 70

	Wet bulk density (gm/cm³)	Grain density (gm/cm³)	Porosity (%)	Compressional wave velocity (km/sec)	Thermal conductivity (W/mK)
Manganese oxides	1.98 ± 0.26	3.75 ± 0.36	64.0 ± 10.3	2.22 ± 0.07	..
Granular green clays	1.46 ± 0.19	3.13 ± 0.23	77.9 ± 8.5	1.61 ± 0.09	0.80 ± 0.07
Nongranular green clays	1.20 ± 0.10	2.74 ± 0.28	89.8 ± 5.4	1.55 ± 0.02	0.78 ± 0.05
Pelagic sediments	1.32 ± 0.09	2.65 ± 0.08	82.2 ± 4.2	1.51 ± 0.02	0.91 ± 0.08

are least porous. An exception is the nongranular green clays, which were the most porous sediment and, as a result, had the lowest wet bulk densities and thermal conductivities.

The differences among the various sediment properties cause irregular variations in physical properties with depth in holes where both pelagic and hydrothermal sediments were cored (Holes 506, 506C, 506D, 507D, 509B). In contrast, the properties of pelagic sediments, whether or not interbedded with hydrothermal materials, vary smoothly with depth, in a linear fashion similar for all holes. There are no obvious contrasts to account for regional seismic reflectors at 7 and 15 m depth (Lonsdale, 1977).

In the thin sediment cover at Sites 506 to 509, the depth gradient of porosity in the pelagic oozes is very high, about −0.2 to −0.6%/m (see Fig. 6). As a result, gradients in wet bulk density (0.2 to 0.6%/m) and thermal conductivity (0.5 to 1%/m) are also quite high, compared to those in thicker pelagic sections (Hamilton, 1976). In Hole 510, with 110 m of sediments, the gradients in physical properties are "normal" in the upper section, but *near basement* (within 30 m), they become higher and comparable to those of Sites 506 to 509. The occurrence of these high, near-basement depth gradients of physical properties in pelagic sediments in every hole cored on Leg 270 suggests that they are related to some regional sediment-basement interaction near the spreading center, as opposed to a more general physical process such as compaction. The preservation of these high gradients in pelagic layers interbedded with hydrothermal deposits implies that the creation of hydrothermal sediments has little effect on the properties of adjacent pelagic sediments.

Paleomagnetism

A whole-core spinner magnetometer was used on board D/V *Glomar Challenger* to measure the horizontal component of natural remanent magnetism (NRM) of unsplit HPC sections of sediments recovered at Sites 506, 507, and 509. As expected, no reversals were observed at any of these sites, all of which are younger than the 0.72 m.y. age assigned to the Brunhes/Matuyama reversal boundary. Whenever lithologic transitions occurred within undisturbed cores, no significant differences were observed between remanence directions and intensities of the pelagic oozes and hydrothermal clays. These preliminary measurements thus suggest either that the deposition of the hydrothermal clays and pelagic oozes was penecontemporaneous, or, if the nontronitic clays were formed later by hydrothermal activity, that the magnetic oxides responsible for the magnetic remanence of the sediments were not significantly altered.

Mn-oxide fragments from Hole 509B exhibit an unusually weak magnetization intensity, $\bar{J}_{NRM}$, consistently less than 1 x 10^{-6} Gauss, which is about an order of magnitude less than that of the nontronitic clays. These low $\bar{J}_{NRM}$ values are consistent with the results of DSDP Leg 54, which showed that the Mn-oxide fragments are depleted of iron (Hekinian and others, 1978). However, the relative declinations are surprisingly well clustered, suggesting the presence of a small fraction of a remanence-carrying phase or phases.

BASEMENT ROCKS

Petrography

Drilling of basalt was attempted in 13 holes representing all of the sites occupied in the Galapagos. Loose rubble and/or highly fractured rock was encountered at the sediment-basalt interface at all sites. The difficult drilling into such material resulted in low total penetration and recovery (approximately 15%).

Young crust at Sites 506, 507, and 508 yeilded nearly identical samples of fine- to medium-grained, aphyric to sparsely plagioclase phyric basalt. Textures range from glassy to ophitic/intergranular. Plagioclase is the dominant phenocryst phase (<5%) with very subordinate clinopyroxene (<3%?). Microlites and small crystals of plagioclase and clinopyroxene comprise the interstitial matrix and form quenched textures. Titanomagnetite, which comprises 8% to 13% of the nonglassy samples, is the dominant opaque phase and appears to be fresh. Primary spherules of sulfide minerals, never exceeding 1%, accompany the titanomagnetite.

At Site 510, fine- to medium-grained, moderately (2% to 10%) plagioclase-rich, sparsely (1% to 2%) olivine phyric basalt was recovered. Titanomagnetite is less abundant at Site 510 than at Sites 506 to 508, ranging from 3% to 8% of the rock.

Comparisons of the phenocryst assemblages, Fe-Ti oxides, and chemical analyses show that the young basalts recovered near the spreading center on Leg 70 are derived from ferrobasaltic magmas, whereas intermediate-aged basalts are typical oceanic tholeiites. Ferrobasalts and fractionating plagioclase and clinopyroxene have been postulated as erupting from rather shallow magma reservoirs below the Galapagos spreading center (Schilling and others, 1976; Clague and Bunch, 1976).

Alteration

Most of the basalt samples from Site 506 appear to be fresh, but a few samples are

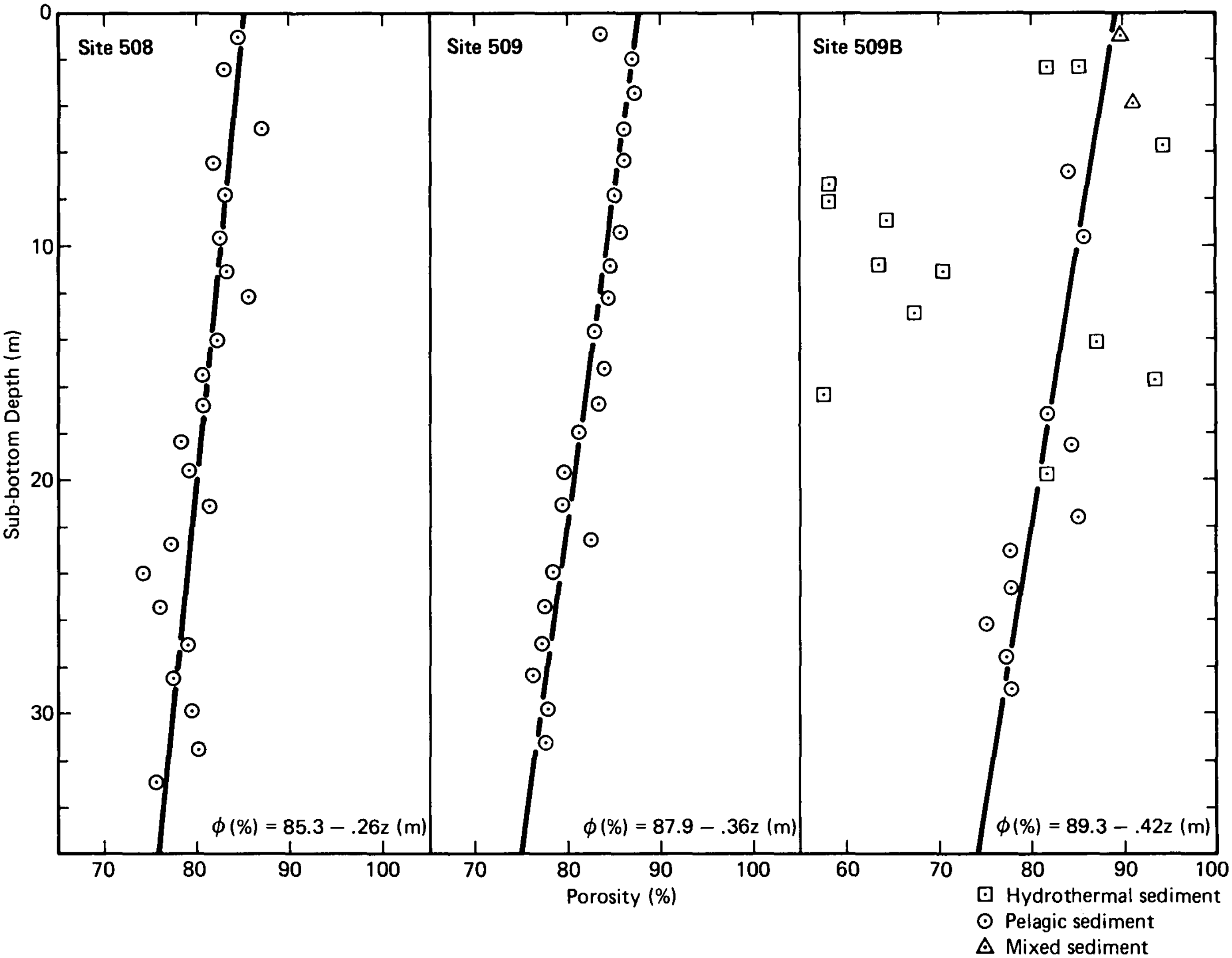

Figure 6. Porosity measurements versus depth with linear regressions for three representative holes: low heat-flow, non-mound Site 508; high heat-flow, off-mound Site 509; pelagic ooze samples only.

slightly altered, as indicated by the presence of smectite in vesicles and interstitital voids. A thin (less than 4 mm) rim occurs in a few samples (Fig. 7).

At Site 507, the basalt texture clearly influences the alteration. The subophitic basalts seem to be fresh, whereas the hyalopilitic basalts are altered and show dark alteration rims (average thickness, 8 mm; maximum thickness, 15 mm) subparallel to exposed surfaces and fissures. These alteration rims correspond to vesicles and miarolitic voids infilled by alteration minerals. These are, in order from the exposed surface to the centers of the samples: (1) iron oxyhydroxides, (2) green smectite (in the rims of vesicle infillings) and (3) iron oxyhydroxides (in their centers); (4) green smectite. All of the voids in the centers of the samples are empty.

At Site 508, all of the samples exhibit altered rims, sometimes up to 50 mm thick. Alteration mineral zonation was observed as follows, from the exterior to the center of the samples: (1) iron oxhydroxides + green smectite + brown smectite(?); (2) green smectite; (3) brown smectite. Empty voids are always found in the centers of the fresher appearing samples. A drusy mineral, possibly a zeolite, has been observed in some vesicles.

At Site 510, the thickness of the alteration rims ranges from 5 to 40 mm, averaging roughly 15 mm. Alteration also appears to be controlled by fissures, cracks, and exposed surfaces. In the alteration rims, the pore spaces are often filled by the following secondary mineral sequence, starting from the exposed surface to the core of the sample: (1) bright green smectite, (2) brownish-green smectite, (3) very pale brown smectite. Secondary mineral sequences are sometimes more complex. For instance, the following paragenetic succession from the rock interior through an alteration rim was observed adjacent to a smectite veinlet: (1) $Fe(OH)_n$ (not always present), (2) orange-brown smectites with $Fe(OH)_n$, (3) mixed orange-brown and green smectites (and possible calcite), (4) green smectite (and possible zeolite), (5)

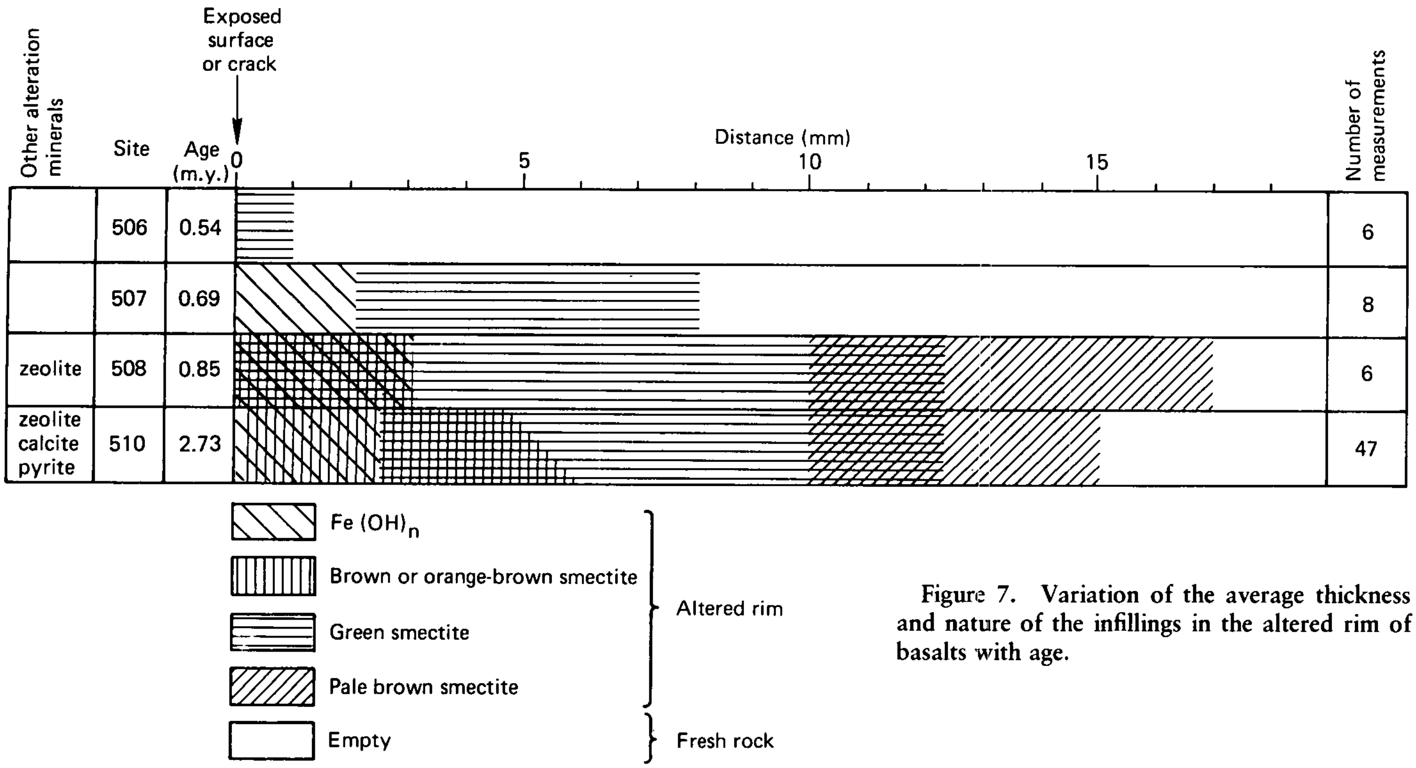

Figure 7. Variation of the average thickness and nature of the infillings in the altered rim of basalts with age.

very light brown smectite. A secondary mineral paragenetic succession in another veinlet from pyrite along the walls, through various smectites to Fe-oxyhydroxides in the center, indicates that the conditions changed from anoxic to oxic or suboxic.

Figure 7 illustrates the variation in the secondary mineral paragenetic sequence with age observed in alteration rims of Galapagos basalts. This figure shows that the mean widths of the alteration rims increase with age from Site 506 to 508, that is, between 0.55 and 0.85 m.y. Alteration minerals can be readily explained by the interaction between basalt and sea water at low temperature, although some higher temperature hydrothermal alteration may also be invoked.

Physical Properties

Due to the low recovery of basalts, shipboard physical property measurements were carried out on only a limited number of samples (wet bulk density and sonic-velocity measurements for 21 samples, grain density and porosity measurements for 12 samples). The results are summarized in Table 2. On the average, the Galapagos basalts have high grain densities and low porosities and, as a result, high wet bulk densities, compared with those of other areas (for example, Site 417, Atlantic Ocean floor).

Paleomagnetism

Table 3 summarizes the results of paleomagnetic measurements of basement basalt samples carried out on board D/V *Glomar Challenger*. The NRM intensity of the natural remanent magnetization, $\bar{J}_{NRM}$, is of key importance for modeling the thickness of the layer responsible for the marine magnetic anomalies. There is no significant difference between $\bar{J}_{NRM}$ at the youngest Site 506 and at those of intermediate age, Sites 507 and 508. $\bar{J}_{NRM}$ is approximately equal to 22×10^{-3} Gauss for Sites 506, 507, and 508. This value is extremely high relative to other oceanic basalts, especially considering the equatorial location of the sites, and, indeed, it is comparable to values of new crust in the FAMOUS area of the Mid-Atlantic Ridge (Johnson and Atwater, 1977). Furthermore, $\bar{J}_{NRM}$ value for these sites is very similar to the value of 25×10^{-3} Gauss used by Sclater and Klitgord (1973) to model the central anomaly. Thus, it appears that the assumption of a 500-m-thick magnetized layer to explain the observed anomalies is a rather good approximation in this area.

Despite its relatively high value, $\bar{J}_{NRM}$ of Sites 506, 507, and 508 is only about one-half that of zero age samples from the Galapagos spreading center, just 19 to 26 km north of these sites (Anderson and others, 1975; Levi, unpub. data). The precise cause of the decrease of $\bar{J}_{NRM}$ relative to that at the spreading center must await further study. However, previous work in the Atlantic Ocean (Irving and others, 1970) has shown that low-temperature oxidation of the primary titanomagnetite is an important mechanism for the decrease of $\bar{J}_{NRM}$ with distance (age) from the spread-

TABLE 2. DENSITY, POROSITY, AND SONIC VELOCITY OF GALAPAGOS BASALTS, LEG 70

	Wet bulk density (gm/cm³)	Grain density (gm/cm³)	Porosity (%)	Sonic velocity (km/sec)
"Young" Galapagos (Sites 506, 507, 508)	2.94 ± 0.03	3.05 ± 0.03	4.8 ± 1.1	5.26 ± 0.28
"Old" Galapagos (Site 510)	2.95 ± 0.03	3.00 ± 0.02	3.6 ± 0.8	5.68 ± 0.16
All sites	2.94 ± 0.03	3.02 ± 0.03	4.2 ± 1.1	5.47 ± 0.31

TABLE 3. SUMMARY OF MAGNETIC RESULTS FOR BASALT SAMPLES FROM NEAR THE GALAPAGOS SPREADING CENTER, LEG 70

Site	Age of crust	$\bar{J}_{NRM}$ ($\times 10^{-3}$ Gauss)	$\bar{X}$ ($\times 10^{-3}$ Gauss/De)	$\bar{Q}$	$\overline{MDF}$ (Oersted)	$\bar{I}_{NRM}$ (°)	$\bar{I}_{STABLE}$ (°)
506	0.54 m.y.	22.1 ± 9 (8)	1.51 ± .51 (8)	53 ± 32 (8)	156 ± 44 (4)	−17 ± 12 (7)	−21 ± 17 (4)
507* 508*	0.69 m.y. 0.85 m.y.	20.8 ± 12 (6)	2.13 ± .80 (6)	35 ± 25 (6)	135 ± 64 (5)	2 ± 12 (4)	8 ± 0 (2)
510	2.73 m.y.	6.3 ± 4 (18)	0.97 ± .35 (18)	22 ± 14 (18)	180 ± 90 (8)	−13 ± 7 (17)	−16 ± 4 (7)

* Data for Sites 507 and 508 are combined.
Uncertainties represent one standard deviation. Numbers in parentheses designate the number of samples used in obtaining mean values.

ing axis. $\bar{J}_{NRM}$ at Site 510 is less than one-third of that at the younger sites, and this is thought to be too much of a decrease to be accounted for entirely by progressive low-temperture oxidation. Preliminary petrographic observations indicate that the Site 510 basement rocks are not ferrobasalts. Hence, Site 510 is just outside the zone of the high-amplitude magnetic anomalies.

Q, the ratio of remanent to induced magnetization, is high at all sites, indicating the dominance of the remanent with respect to the induced magnetization, a finding consistent with the existence of distinct magnetic anomaly profiles. Q progressively decreases with age. However, this trend is not repeated by the MDF (median demagnetizing field) values. The relatively high MDF values suggest that the remanence at all four Galapagos sites resides in fine particles of titanomagnetite. The stability of the remanence is further demonstrated by the small change in remanence direction upon AF (alternating field) demagnetization.

The shallow inclinations of samples from all four sites are consistent with the sites' equatorial locations. The present inclination at the sampling sites is about +21°, and that expected from a geocentric axial dipole is very near zero.

HEAT FLOW

Downhole sediment temperatures were successfully measured by a probe penetrating undisturbed sediments below the drill bit immediately adjacent to several HPC holes at Sites 506 to 509, and during the process of drilling the single hole at Site 510. The results are summarized in Table 4. Temperatures were determined by monitoring the resistance of a single thermistor, intruding about 1 m into the sediment, to a precision of 10 ohms, providing a nominal temperature resolution of about 0.01 °C. At Sites 506 through 509, two or three stops were characteristically made at 8- to 10-m intervals for temperature determinations in the ~ 30-m-thick sediment columns. In most cases, the estimated precision of the measured thermal gradients is 0.05–0.1 °C/m, due to several sources of experimental error. Among these are inaccuracies in determining and maintaining the probe position to better than ±1 m relative to the sediment-water interface and errors in the temperature observations resulting from some combination of instrument drift, possible water circulation about the probe, and probe motion due to the low shear strength of the sediments. Normally, such imprecision in gradients would produce large uncertainties in heat-flow values, but in this area of high-heat flow, it results in errors of only 5% to 10%.

Sediment thermal conductivities were measured on board the D/V *Glomar Challenger* at close intervals (1 to 2 m) in all cores by the needle-probe method (von Herzen and Maxwell, 1959) and were corrected to *in situ* conditions using the relation of Ratcliffe (1960), as modified by

TABLE 4. LEG 70 GALAPAGOS SPREADING CENTER HEAT FLOW RESULTS

Measurement hole	Nearest corresponding drill hole(s)	Thermal conductivity (z = metres of sediment) W/mK	Surface heat flow mW/m²	Thermal regime
506E	506 (mound)	.79 + .005z	1276 ± 100	Discharge 1.6-1.8 × 10^{-6} cm/sec (~52 cm/yr)
506F	506B (off-mound)	.72 + .015z	552 ± 30	Conductive
507A	507, 507B (off-mound)	.76 + .009z	585 ± 40	Discharge 3-5 × 10^{-7} cm/sec (~12 cm/yr)
507E	507D (mound)	.66 + .009z	334 ± 40	Conductive
507G	507F (mound?)	.76 + .009z	481 ± 25	Conductive (possible slow discharge of $<10^{-7}$ cm/sec)
507I	507H (off-mound)	.79 + .007z	364 ± 20	Conductive
508A			85 ± 10	Recharge 1.1-1.3 × 10^{-6} cm/sec (~38 cm/yr)
508D	508 (pelagic)	.78 + .007z	225 ± 10	Conductive
508E			83 ± 10	Recharge 1.4-1.6 × 10^{-6} cm/sec (~47 cm/yr)
509C	509B (mound)	.72 + .011z	1072 ± 80	Discharge (7-9 × 10^{-7} cm/sec (~27 cm/yr)
509D	509 (off-mound)	.74 + .010z	501 ± 125	Conductive (irregular gradient)
510	510 (pelagic)	.89 + .06 z (z < 100 m) .80 + .005z (z > 65 m)	184 ± 10	Conductive

Note: Estimated uncertainties in surface heat flow reflect two major sources of error: a 5% uncertainty in thermal conductivity values and variable errors in the determination of thermal gradients.

Hyndman and others (1974). Equipment uncertainties limited the accuracy of shipboard conductivity measurements to ±10%; previously reported values average about 5% lower than ours, which may therefore be as much as 5% too high. Nevertheless, the relative variation of conductivity, both among sites and downhole, was well determined. At each site, conductivities were found to increase rapidly with depth within 30 to 50 m of basement, with a gradient of about 0.20 mcal/cm-sec-°C/m (0.01 W/mK/m). Linear increases of thermal conductivity with depth fit the data significantly better than do mean values, and hence were used in calculating heat flows. For a constant conductive heat flow, this linear increase of conductivity with depth should be coupled with a corresponding decrease in the temperature gradient with depth. Indeed, most temperature profiles were found to be non-linear with depth, but not always in the sense required for purely conductive heat flow. These nonconductive, nonlinear profiles were fit to a steady state, one-dimensional fluid flow equation (Bredehoeft and Papadopulos, 1965), modified for the depth variation of conductivity, to yield the apparent pore-water flow rates given in Table 4. These values are probably no better than order of magnitude estimates; nevertheless, we believe that they reflect real differences in the thermal processes occurring at the various mounds and pelagic core sites.

Despite the relatively large measurement uncertainties, our heat-flow values agree well with detailed surface heat-flow contours based on several hundred short probe measurements in the immediate area (Sclater and Klitgord, 1973; Williams and others, 1974; Green and others, 1981). The deeper penetration of our measurements gives better resolution of fluid flow processes in sediments. These processes may be coupled to those in the more permeable basement rocks inferred to be responsible for the regular variation of heat flow at the Galapagos spreading center.

The heat-flow values in the vicinity of mounds are very high. Temperature profiles at three (506, 507, 509B) of the five mounds measurement holes are distinctly nonlinear and display a sense consistent with convective hydrothermal discharge at rates of the order of 10^{-6} cm/s (30 cm/yr). The other two mound holes (507D, 507F) have mostly conductive heat flows, with hints of discharge at slower rates (10^{-7} cm/s), which are beyond the resolution of our measurements. None of our other measurements displayed this type of nonlinearity. At all three mound sites (506, 507, and 509), holes drilled in pelagic sediments nearby (0.1 to 0.5 km), but off the mounds, had conductive temperature profiles, indicating that the apparent hydrothermal discharge is quite localized, as has been proposed in models of this process (Spooner and Fyfe, 1973; Lonsdale, 1977) and observed in hydrothermal fields such as the Reykjanes Peninsula in Iceland (Palmason, 1967).

At the low heat flow site (508), where only pelagic sediments were cored, three heat flow measurements made quite close together gave somewhat conflicting results. Surface heat flows were relatively low, but ranged from 1.7 to 5.5 HFU (70–230 mW/m^2). Two of the three temperature profiles (Holes 508 and 508E) were strongly non-linear and displayed a sense consistent with recharge (downward flow of bottom water through the sediments) at rates of the order of 10^{-6} cm/s (30 cm/yr). The association of downward water flow with relatively low heat flow supports the inference of convective recharge at heat flow minima in a cellular pattern (Williams and others, 1974; Green and others, 1981).

DISCUSSION

Here we anticipate one of our conclusions that the survey data and observations collected to date, and preliminary results of our drilling, do not yet allow a unique model of formation of the Galapagos mounds. The models of mounds that are developed, however must be constrained by all existing data. In the following, we summarize the relevant observations made over the past decade on these mounds.

1. The mounds are located 20 to 30 km south of the Galapagos Spreading Center over crust 0.5 to 0.9 Ma in age, where the sediment is 25 to 50 m thick. Mounds are not found over younger crust to the north, although some mounds may be buried by thicker sediments on older crust to the south. The mounds are found only on the south flank of the Galapagos Spreading Center, although appropriate near-bottom survey data are hardly adequate on the north flank.

2. The mounds are frequently located over small (≤ few metres) vertical displacements of the upper basement rock surface (Lonsdale, 1977).

3. The mounds are located in a region of high heat flow (8 to 10 HFU), with extremely high and localized heat flow (10^2-10^3 HFU) associated with some mound peaks (Williams and others, 1979). Our data show that nonlinear temperature and chemical gradients are generally of a distinctive character between *on* and *off* mounds sites, usually concave *downward* in the former and concave *upward* in the latter. We interpret these profiles to indicate an upwelling of hydrothermal solutions through the entire mounds region. These solutions may be rising one or two order of magnitude more rapidly in the mounds proper than in the sea floor surrounding the mounds.

4. Although temperatures up to 15 °C were measured within the mounds, extensive surveys show no measurable active hydrothermal venting over mounds, unlike the spreading center to the north (Corliss and others, 1979a).

5. As observed from bottom photographs and submersibles, mound surfaces are comprised of acoustically reflective Mn-oxide crusts, with associated iron oxides and smectites of yellow or orange color (Corliss and others, 1978; Williams and others, 1979).

6. The sedimentary stratigraphy of mounds determined from cores recovered during DSDP Leg 70 drilling is consistently grouped in three units, from uppermost to lowermost: (a) a siliceous foraminifer nannofossil ooze, usually capped with a surface layer of "oxidized" pelagic mud, and generally overlying, with a sharp contact; (b) interbedded pelagic and hydrothermal sediments, which always progressively grade downwards into (c) a foraminifer nannofossil ooze, underlain by basement.

7. The biogenic siliceous component of pelagic sediments decreases more rapidly with depth at mounds sites than at off-mounds sites.

8. The hydrothermal layers of unit b lack carbonate and siliceous organisms, and their composition is similar to those of equivalent nontronitic clays and Mn-oxides which have been ascribed to hydrothermal activity near the Galapagos spreading center and at other locations of the world rift system (Bischoff, 1972; Corliss and others, 1978; Scott and others, 1974; Moore and Vogt, 1976; Hoffert and others, 1978; Hoffert and others, 1981).

9. The bulk of the hydrothermal material is confined both vertically and horizontally within the vicinity of the mounds.

10. Although recovery was poor, the

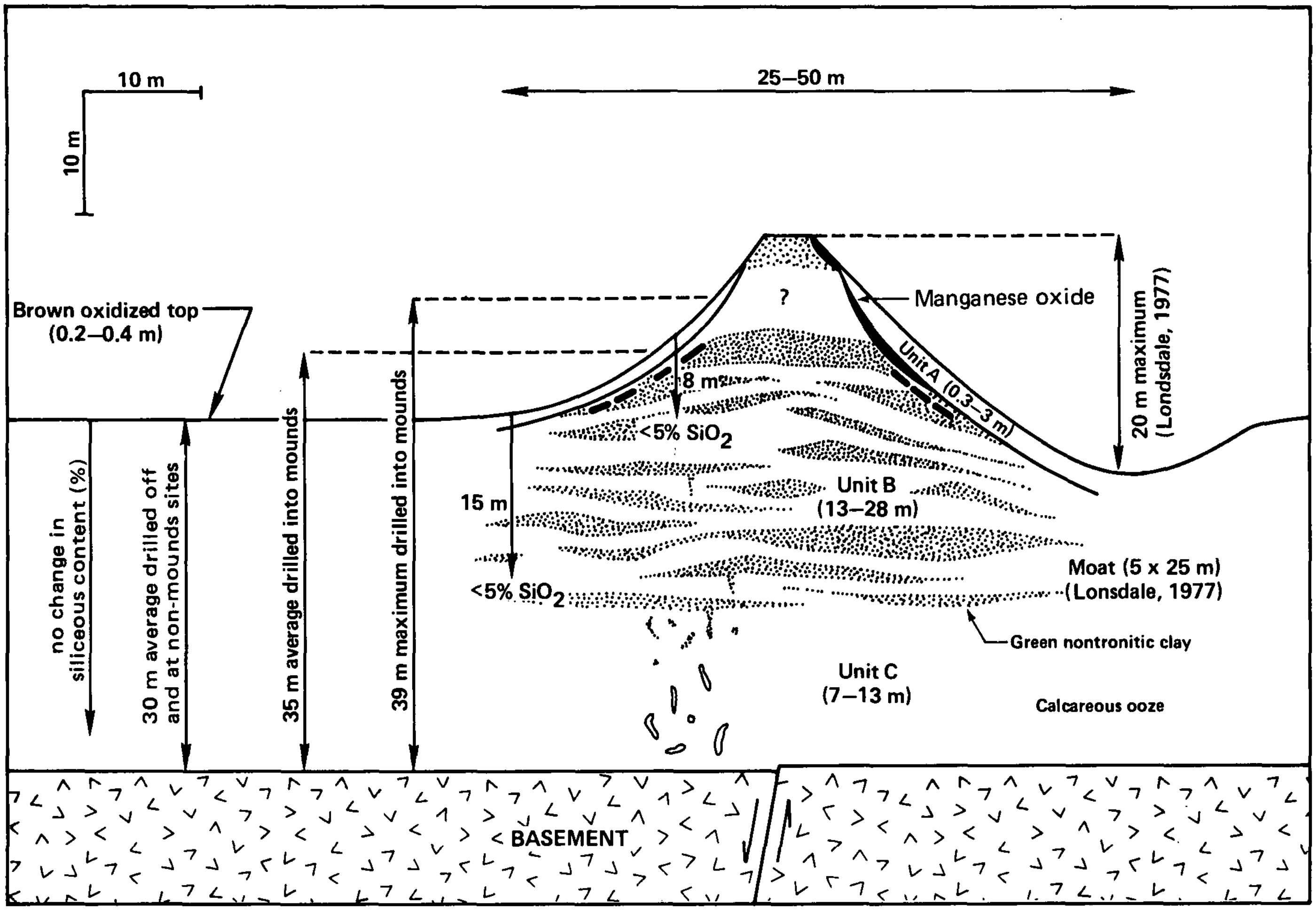

Figure 8. Idealized geometry of the Galapagos hydrothermal mounds.

uppermost few metres of basement rock, drilled both on and off mounds, shows little evidence of any high temperature hydrothermal alteration.

Most of these observations lead us to models of mounds formation as a result of precipitation of materials from hydrothermal solutions, as others have previously deduced (Klitgord and Mudie, 1974; Lonsdale, 1977; Corliss and others, 1978; Williams and others, 1979). However, the unique results of our mounds drilling allows us to narrow the range of specific models.

The presence of pelagic sediments as the most superficial mound layer in all of the DSDP cores would imply that the hydrothermal activity has ceased. This inference is inconsistent with the observation of the submersible that hydrothermal products crop out at mound tops and with the high water temperature measured above the mounds, and with the shipboard heat-flow measurements and pore-water analyses indicating rapid upwelling of hydrothermal solutions through the mounds. The apparent contradiction is removed if the mound cores were drilled into the flanks and not the tops of active mounds. The nonlinear chemical and thermal gradients also strongly suggest that mounds are actively forming at present, rather than being relics of some past local geological event. The high heat flow surrounding the region of mounds, and even higher heat flows on some mounds, are consistent with a model of upward-moving hydrothermal solutions.

Our physical model, then (Fig. 8), is one of slowly upward percolating hydrothermal fluids through sediments, which interact chemically with the sediments and sea water to form mounds by precipitation of hydrothermal minerals. The mounds are formed above localized regions of the crust with higher permeability where the rubble-like thin lava flows of the basement have been further disrupted by faulting.

The restricted distribution of the hydrothermal products and their interfingering with the mounds pelagic sediments, combined with the evidence for gradational contacts, indicate that intimate interactions between these two materials occurred beneath the water-sediment interface. The direct discharge of hydrothermal solutions into sea water to form the hydrothermal products by precipitation onto the sea floor, as suggested by Hekinian, Rosendahl, and others (1977), seems less likely.

It has been proposed that the nontronitic clay mineral formed first (Bischoff, 1972; Rateev and others, 1981) and this mineral was later progressively replaced by a celadonite, or vice versa (Hoffert and others, 1978, 1981). Alternatively, iron could precipitate first in pelagic sediments as amorphous Fe-oxhydroxides from upward-diffusing hydrothermal waters and the Fe-oxhydroxides further react with the hydrothermal solutions and the biogenic silica to form nontronite.

Charge-balance considerations put useful constraints on how the iron in the hydrothermal solutions is converted into Fe-oxhydroxides or nontronite in the mounds. On the one hand, the iron in the ascending solutions is most probably reduced, Fe^{3+} being insoluble except in very acidic solutions. On the other hand, the iron in Fe-oxyhdroxides or nontronite is completely or mainly trivalent, and $Fe_4Si_8O_{20}(OH)_4$ can be taken as a simple formula of this clay mineral. Therefore, an essential component of nontronite formation is the oxidation of Fe^{2+}. Three oxidants are capable of energetically oxidizing ferrous iron: O_2, NO_3^- and MnO_2. The over-all reaction involving O_2 is:

$$4Fe^{++} + 8SiO_2 + O_2 + 6H_2O \rightarrow Fe_4Si_8O_{20}(OH)_4 + 8H^+. \quad (1)$$

One mechanism for oxidation is the downward diffusion of O_2 and/or NO_3^- from the sediment-water interface. For normal diffusion rates, calculations show that nontronite would have to be forming within a few centimetres of the interface to match the sedimentation rate in this region (5 cm/10^3yr). The calculations for reasonable concentrations of oxidants in bottom water [$(O_2) = 10^{-4}M$, $(NO_3^-) = 0.4 \times 10^{-4}M$] give required water fluxes of a few tens of centimetres per year, rates which are quite consistent with measured temperature and chemical gradients.

An important feature of reaction 1 is that protons (H^+) are produced which can drive calcite dissolution according to the following equation:

$$4Fe^{++} + 8SiO_2 + O_2 + 6H_2O + 8CaCO_3 \rightarrow Fe_4Si_8O_{20}(OH)_4 + 8Ca^{++} + 8HCO_3^- \quad (2)$$

Similar reactions can be formulated for NO_3^- and MnO_2 reduction. The generation of acid during nontronite formation presumably drives the dissolution of $CaCO_3$ and helps account for the purity of the nontronite in the sediments. If nontronite is formed by oxygen reduction, for example, 8 moles of $CaCO_3$ (with a sediment volume of 1,500 cm^3) are dissolved per mole of nontronite produced (with a volume of 900 cm^3), resulting in a 40% volume reduction of the sediment column. This might explain the presence of the moats around mounds.

The lack of biogenic SiO_2 in mounds sediments may also be a result of dissolution by ascending solutions. Calculations show that pore waters ascending at rates of a few tens of centimetres per year can dissolve all of the silica at the present rate of accumulation if they acquire silica in solution with a concentration of a few hundred $\mu M\ \ell^{-1}Si$. It is not clear yet whether the siliceous and/or carbonate microfossils are being dissolved or replaced by the nontronite. Studies of sectioned sediment samples with a transmission electron microscope presently in progress should help to determine whether nontronite coats and fills the microfossil debris, or substitutes for their skeletons, or both.

The evidence uniquely provided from drilling that MnO_2 generally overlies nontronite suggests a mechanism for nontronite formation by replacement of MnO_2 accompanied by $CaCO_3$ dissolution according to the following equation:

$$4Fe^{++} + 8SiO_2 + 2MnO_2 + 4H_2O + 4CaCO_3 \rightarrow Fe_4Si_8O_{20}(OH)_4 + 2Mn^{++} + 4Ca^{++} + 4HCO_3^- \quad (3)$$

A similar equation can be developed for reduction of NO_3^-. This could be accomplished by either continuous, or sudden (batch) replacement of MnO_2 by nontronite. The continuous upward growth of nontronite at the expense of MnO_2 would account for the scarcity of MnO_2 crusts at depth in the mounds sediments. The interlayering of pure nontronite and pelagic sediments may be better explained by batch replacement by nontronite.

Our observations can be explained in terms of either a steady-state process or an episodic process with hydrothermal minerals forming during brief intervals, perhaps once every 10^4 to 10^5 yr. We infer from the presence of 10 m or so of basal carbonate ooze at mounds sites that hydrothermal minerals began to form at least about 200,000 yr after the onset of sediment accumulation. If mounds formation is a steady-state process of the Galapagos region, this implies that incipient mounds may be found as close as 7 km from the spreading center, assuming a half spreading rate of 3.5 cm/yr (Klitgord and Mudie, 1974). However, the region out to about 15 km from the spreading center is predominantly characterized by relatively low heat flow and thin sediments, which may delay initiation of mounds formation until 400,000 yr or so. Moreover, if one assumes that the nontronite formed by reaction with and replacement of the pelagic sediments, then the hydrothermal process started after the pelagic components of both Units b and c had been deposited, that is, about 400,000 yr. In this case, the age of mounds hydrothermal material should range from present to a few 10,000 yr.

Very high gradients in sediment physical properties occur within 30 to 50 m of the basalt basement at Sites 506-510. It is interesting that this is also the sediment thickness where mounds are presently found, and this similarity may not be coincidental. The large physical properties gradients may be interpreted as a rapid dewatering, or another process which reduces porosity, of the earliest sediments deposited on young ocean crust. As proximity to basement seems to be the controlling factor, it seems logical to associate this effect with hydrothermal circulation. The 30 to 50 m sediment thickness may be the critical thickness at which hydrothermal solutions can effectively interact with the sediments in the Galapagos (Williams and others, 1979). For younger crust with thinner sediments, the hydrothermal fluids may exchange with sea water primarily through permeable rock outcrops, bypassing less permeable sediments. On older crust, exchange of hydrothermal waters with sea water may be effectively suppressed by thicker sediments. In any case, although the exact cause of the physical properties gradients is not determined, the association of mounds formation with sediment thicknesses comparable to those in which large physical properties gradients occur suggests a common origin for both.

From shipboard physical properties measurements on disturbed mounds sediments, Hekinian, Rosendahl, and others (1977) concluded that the green-clay sediments were denser and had higher *in situ* (?) sonic velocities than the associated pelagic oozes. The two reflectors that Lonsdale (1977) attributed to ash layers were interpreted by Natland and others (1979) as corresponding to the contrast between the top and bottom of the green smectite layer and the pelagic sediments. As a consequence, this "hydrothermal" layer was believed to extend continuously throughout the mounds field and, indeed, throughout the entire region. We found only one ash layer in one of our cores, and the regional extension of nontronitic clay layers, as well as a drastic change in the sediment phsycial properties must be excluded as sources of the reflectors. We are unable, at this stage, to suggest any alternative explanation.

CONCLUSIONS

The successful drilling and sampling of the Galapagos hydrothermal mounds on Leg 70 has provided many new data on their nature and origin. The most important conclusions from these data are the following:

(1) The hydrothermal sediments contained in the mounds are limited in lateral distribution to the immediate vicinity (≤100 m) of the mounds or mound ridges. (2) The stratigraphy of the hydrothermal deposits, composed primarily of Mn-oxides overlying nontronite, both interbedded with and sandwiched between pelagic sediments, narrows the range of acceptable models of mounds formation. The slow interaction of hydrothermal solutions with pelagic sediments is preferred, rather than rapid debouchment of hydrothermal sediments onto the sea floor. (3) Thermal and chemical gradients in the sediments on and near the mounds indicate that hydrothermal solutions are presently active in the formation of the mounds. The mounds form in a few $\times 10^5$ years or less. (4) The lack of hydrothermal alteration of the uppermost few metres of basement rocks in the Galapagos area is consistent with the generally low temperatures (≤25°C) presently found there. The hydrothermal solutions must tap much deeper (≥1 km) rocks at higher temperatures.

ACKNOWLEDGMENTS

The successful program of mounds drilling on Leg 70 obviously depended entirely on the expertise provided by the officers and crew of the D/V *Glomar Challenger,* operated by Global Marine Inc. under contract to the University of California. The nearly flawless operation of the hydraulic piston corer, developed at the Deep Sea Drilling Project, was also crucial to our success. Mr. Robert Knapp, DSDP Operations Manager for Leg 70, provided the valuable expertise required for the smooth functioning of a complex operation.

We are grateful to James Hall and the JOIDES Ocean Crust Panel for initiating and sponsoring this program.

REFERENCES CITED

Allmendinger, R. W., and Riis, F., 1979, The Galapagos rift at 86°W: Regional morphological and structural analysis: Journal of Geophysical Research, v. 84, p. 5379–5389.

Anderson, R. N., Clague, D. A., Klitgord, K. D., Marshall, M., and Nishimori, R. K., 1975, Magnetic and petrologic variations along the Galapagos spreading center and their relation to the Galapagos melting anomaly: Geological Society of America Bulletin, v. 86, p. 683–694.

Bischoff, J. L., 1972. A ferroan nontronite from the Red Sea geothermal system: Clays and Clay Mineralogy, v. 20, p. 217–223.

Bredehoeft, J. D., and Papadopulos, I. S., 1965, Rates of vertical ground water movement estimated from the Earth's thermal profile: Water Resources Research, v. 1, no. 2, p. 325–328.

Clague, D. A., and Bunch, T. E., 1976, Formation of ferrobasalt at East Pacific mid-ocean spreading center: Journal of Geophysical Research, v. 81, p. 4247–4256.

Corliss, J. B., Lyle, M., Dymond, J. R., and Crane, K., 1978, The chemistry of hydrothermal sediment mound deposits near the Galapagos rift: Earth and Planetary Science Letters, v. 40, p. 12–24.

Corliss, J. B., Dymond, J. R., Gordon, L. I., Edmond, J. M., von Herzen, R. P., Ballard, R. D., Green, K., Williams, D. L., Bainbridge, A., Crane, K., and van Andel, Tj. H., 1979a, Submarine thermal springs on the Galapagos rift: Science, v. 203, p. 1073–1083.

Corliss, J. B., Gordon, L. I., and Edmond, J. M., 1979b, Some implications of heat/mass ratios in Galapagos rift hydrothermal fluids for models of sea water-rock interaction and the formation of oceanic crust, *in* Talwani, M., Harrison, C. G., and Hayes, D. E., (eds.), Deep drilling results in the Atlantic Ocean: Ocean crust, Maurice Ewing Series 2: Washington, D.C., American Geophysical Union, p. 391–402.

CRRUST, 1981, Preliminary results from Legs 69 and 70, Deep Sea Drilling Project: Costa Rica rift: Geological Society of America Bulletin, (in press).

Edmond, J. M., Measures, C. McDuff, R. E., Chan, L. H., Collier, R., Grant, B., Gordon, L. I., and Corliss, J. B., 1979a, Ridge crest hydrothermal activity and the balances of the major and minor elements in the ocean: The Galapagos data: Earth and Planetary Science Letters, v. 46, p. 1–18.

Edmond, J. M., Measures, C., Mangum, B., Grant, B., Sclater, F. R., Collier, R., Hudson, A., Gordon, L. I., and Corliss, J. B., 1979b, On the formation of metal-rich deposits at ridge crests: Earth and Planetary Science Letters, v. 46, p. 19–30.

Ewing, J., and Houtz, R., 1979, Acoustic stratigraphy and structure of the oceanic crust, *in* Talwani, M., Harrison, C. G., and Hayes, D. E., ed., Deep drilling results in the Atlantic Ocean: Ocean crust, Maurice Ewing Series 2: Washington, D.C., American Geophysical Union, p. 1–14.

Gartner, S., 1977, Calcareous nannonfossil biostratigraphy and revised zonation of the Pleistocene: Marine Micropaleontology, v. 2 p. 1–25.

Green, K. E., von Herzen, R. P., and Williams, D. L., 1981, The Galapagos spreading center at 86°W: A detailed geothermal field study: Journal of Geophysical Research, p. 979–986.

Hamilton, E. L., 1976, Variation of density and porosity with depth in deep-sea sediments: Journal of Sedimentary Petrology, v. 46, p. 280–300.

Hekinian, R., Rosendahl, B. R., Cronan, D. S., Dmitriev, Y., Fodor, R. V., Goll, R. M., Hoffert, M., Humphris, S. E., Mattey, D. P., Natland, J., Petersen, N., Roggenthen, W., Schrader, E. L., Srivastava, R. K., and Warren, N., 1978, Hydrothermal deposits and associated basement rocks from the Galapagos spreading center: Oceanologica Acta, v. 1, p. 473–482.

Hey, R., Johnson, G. L., Lowrie, A., 1977, Recent plate motions in the Galapagos area: Geological Society of America Bulletin, v. 88, p. 1385–1403.

Hoffert, M., Perseil, A., Hekinian, R., Choukroune, P., Needham, H. D., Francheteau, J., and Le Pichon, X., 1978, Hydrothermal deposits sampled by diving saucer in transform fault "A" near 37°N on the Mid-Atlantic Ridge, FAMOUS area: Oceanologica Acta, v. 1, p. 73–86.

Hoffert, M., Person, A., Courtois, C., Karpoff, A. M., and Trauth, D., 1981, Sedimentology, mineralogy and geochemistry of hydrothermal and sedimentary deposits from Holes 424, 424A, 424B, 424C, *in* Initial reports of the Deep Sea Drilling Project, Volume 54: Washington, D.C., U.S. Government Printing Office, p. 339–376.

Houtz, R., and Ewing, J., 1976, Upper crustal structure as a function of plate age: Journal of Geophysical Research, v. 81, p. 2490–2498.

Hyndman, R., Erickson, A., and von Herzen, R. P., 1974, Geothrmal measurements on Leg 26, *in* Davies, T. A., Luyendyk, B. P., and others, Initial reports of the Deep Sea Drilling Project, Volume 26: Washington D.C., U.S. Government Printing Office, p. 451–463.

Irving, E., Robertson, W. A., and Aumento, S., 1970, The Mid-Atlantic Ridge near 45°N, 6, remanent intensity, susceptibility and iron content of dredged samples: Canadian Journal of Earth Sciences, v. 7, p. 226–238.

Johnson, H. P., and Atwater, T., 1977, A magnetic study of the basalts from the Mid-Atlantic Ridge at 37°N: Geological Society of America Bulletin, v. 88, p. 637–642.

Kaneps, A. G., 1971, Cenozoic planktonic foraminifera from the eastern equatorial Pacific Ocean, *in* van Andel, T. H., Heath, G. R., and others, 1971, Initial reports of the Deep Sea Drilling Project, Volume 16: Washington, D. C., U.S. Government Print-

ing Office, p. 713–745.
Klitgord, K. D., and Mudie, J. D., 1974, The Galapagos spreading center: A near-bottom geophysical survey: Royal Astronomical Society, Geophysical Journal, v. 38, p. 563–586.
Loder, T. C., Lyons, W. B., Murray, S., and McGuinness, H. B., 1978, Silicate in anoxic pore waters and oxidation effect during sampling: Nature, v. 273, p. 373–374.
Lonsdale, P., 1977, Deep-tow observations at the mounds abyssal hydrothermal field, Galapagos rift: Earth and Planetary Science Letters, v. 36, p. 92–110.
Lynn, D. C., and Bonnatti, E., 1965, Mobility of manganese in diagenesis of deep sea sediments: Marine Geology, v. 3, p. 457–474.
Martini, E., 1971, Standard Tertiary and Quaternary calcareous nannoplankton zonation, *in* Faminacci, A., ed., Planktonic Conference, 2nd, Proceedings, Rome, p. 739–785.
Moore, W. S., and Vogt, P. R., 1976, Hydrothermal manganese crusts from two sites near the Galapagos spreading axis: Earth and Planetary Science Letters, v. 29, p. 349–356.
Natland, J., Rosendahl, B., Hekinian, R., Dmitriev, Y., Fodor, R., Goll, R., Hoffert, M., Humphris, S., Mattey, D., Petersen, N., Roggenthen, W., Schrader, E., Srivastava, R., and Warren, N., 1979, Galapagos hydrothermal mounds: Stratigraphy and chemistry revealed by deep sea drilling: Science, v. 204, p. 613–616.
Palmason, G., 1967, On heat flow in Iceland in relation to the Mid-Atlantic ridge, *in* Bjornsson, S., ed., Iceland and mid-ocean ridges, Publication 33: Reykjavik, Society of Science Islandica, p. 111–127.
Ratcliffe, E. H., 1960, The thermal conductivities of ocean sediments: Journal of Geophysical Research, v. 65, p. 1535–1541.
Rateev, M. A., Timofeev, N. V., and Renegarten, N. V., 1981. Minerals of the clay fraction in Pliocene-Quaternary sediments of the east equatorial Pacific, *in* Initial reports of the Deep Sea Drilling Project, Volume 54: Washington, D.C., U.S. Government Printing Office, p. 307–318.
Ross, D. A., Neprochnov, Y. P., and others, 1978, Initial reports of the Deep Sea Drilling Project, Volume 42, Part 2: Washington, D.C., U.S. Government Printing Office, p. 13–15.
Schilling, J. G., Anderson, R. N., and Vogt, P., 1976, Rare earth, Fe and Ti variations along the Galapagos spreading center and their relationship to the Galapagos mantle plume: Nature, v. 261, p. 108–113.
Sclater, J. G., and Klitgord, K. D., 1973, A detailed heat flow, topographic and magnetic survey across the Galapagos spreading center at 86°W: Journal of Geophysical Research, v. 78, p. 6951–6975.
Sclater, J. G., von Herzen, R. P., Williams, D. L., Anderson, R. N., and Klitgord, K., 1974, The Galapagos spreading center: heat-flow low on the north flank: Royal Astronomical Society, Geophysical Journal, v. 38, p. 609–626.
Scott, M. R., Scott, R. B., Rona, P. A., Buttler, L. W.; and Nalwalk, A. J., 1974; Rapidly accumulating manganese deposit from the median Valley of the Mid-Atlantic Ridge: Geophysical Research Letters, v. 1, p. 355–358.
Spooner, E.T.C., and Fyfe, W. S., 1973, Sub-sea floor metamorphism: Heat and mass transfer: Contributions to Mineralogy and Petrology, v. 42, p. 287–304.
von Herzen, R., and Maxwell, A. E., 1959, The measurement of thermal conductivity of deep sea sediments by a needle probe method: Journal of Geophysical Research, v. 64, p. 1557–1563.
Williams, D. L., von Herzen, R. P., Sclater, J. G., and Anderson, R. N., 1974, The Galapagos spreading center: Lithospheric cooling and hydrothermal circulation: Royal Astronomical Society Geophysical Journal, v. 38, p. 587–608.
Williams, D. L., Green, K., van Andel, Tj. H., von Herzen, R. P., Dymond, J. R., and Crane, K., 1979, The hydrothermal mounds of the Galapagos rift: Observations with DSRV Alvin and detailed flow studies: Journal of Geophysical Research, v. 84, no. B13, p. 7467–7484.

MANUSCRIPT RECEIVED BY THE SOCIETY JANUARY 12, 1981